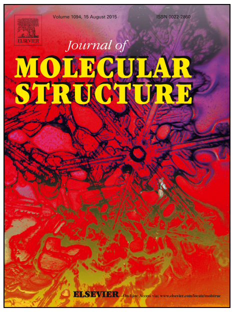

Synthesis, crystal structure and magnetic properties of new trinuclear Copper(II) complexes with Biphenol−Based dinucleating ligands

E. Adelew, K.G. Manoj

PII: S0022-2860(20)30775-4

DOI: https://doi.org/10.1016/j.molstruc.2020.128450

Reference: MOLSTR 128450

To appear in: *Journal of Molecular Structure*

Received Date: 16 December 2019

Revised Date: 11 May 2020

Accepted Date: 13 May 2020

Please cite this article as: E. Adelew, K.G. Manoj, Synthesis, crystal structure and magnetic properties of new trinuclear Copper(II) complexes with Biphenol−Based dinucleating ligands, *Journal of Molecular Structure* (2020), doi: https://doi.org/10.1016/j.molstruc.2020.128450.

First and corresponding Author, Adelew Estifanos Filkale, Ph.D,

- ✓ Designed the schemes
- ✓ Synthesized the compounds
- ✓ Wrote the manuscript
- ✓ Interpreted the results

Coauthor (2nd author) Manuj Kumar Gangwar, Ph.D

- ✓ Solved the crystal structures of the complexes
- ✓ participated in designing and proposing the schemes

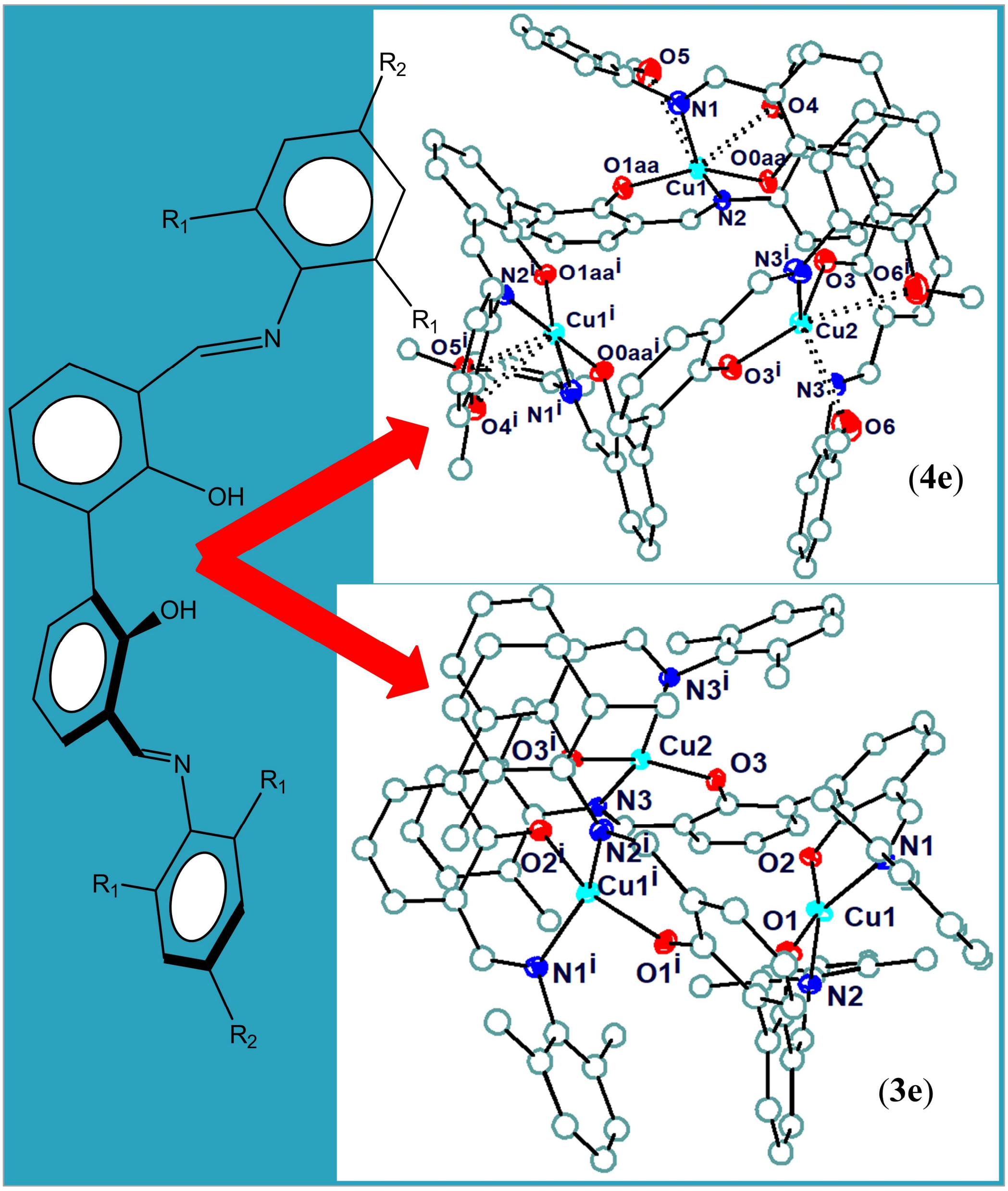
R2
R1
R1
N
OH
OH
N
R1
R1
R2
O5
N1
O4
O1aa
Cu1
O0aa
N2
N2i
O1aai
N3i
O3
O6i
Cu1i
Cu2
O5i
O0aai
O3i
N3
O4i
N1i
O6
(4e)
N3i
O3i
Cu2
O3
N3
N2i
N1
O2i
Cu1i
O2
O1
Cu1
N1i
O1i
N2
(3e)

Synthesis, Crystal Structure and Magnetic Properties of New Trinuclear Copper(II) Complexes with Biphenol–Based Dinucleating Ligands

Adelew. E*, Manoj. K. G.

*Department of Chemistry, College of Computational & Natural sciences, Hawassa University,
P.O. Box, 05, Ethiopia
KAUST Catalysis Center (KCC), King Abdullah University of Science and Technology,
P.O. Box, 4700, Thuwal, 23955-6900, Kingdom of Saudi Arabia.

ABSTRACT

Treatment of (3,3′-*bis*-((2,6-dimethylphenyl)-imino)methyl)-(1,1')-biphenyl-2,2'-diol) (**H_2L^2**) and (3,3′-*bis*-((2-methoxyphenyl))imino)methyl)-(1,1')-biphenyl-2,2'-diol) (**H_2L^3**) with excess $[Cu_2(OAc)_4(H_2O)_2]$ in the presence of triethylamine afforded new trinuclear complexes [Cu(3,3′-*bis*-((R)-iminomethyl)-(1,1')-biphenyl-2,2'-dioxo)]$_3$ [R = 2,6-$Me_2C_6H_3$ (**3e**) and R = 2-$OMeC_6H_3$(**4e**)] respectively. The resulting complexes were characterized by elemental analysis, magnetic susceptibility, EPR, UV-Vis, IR, CV and Single crystal X-ray diffraction analysis. The magnetic susceptibility study of **3e** and **4e** was performed in the 5–300 K and revealed the existence of antiferromagnetic interaction in both complexes. The experimental data could be satisfactorily reproduced using an isotropic exchange model, $H = -J (S_1S_2 + S_2S_3 + S_1S_3)$, yielding as best fit parameters: $J = -15\ cm^{-1}$, $g = 1.99$ for **3e** and $J = -18\ cm^{-1}$, $g = 1.99$ for **4e**. Both complexes have an angular *C*2/c-symmetric trinuclear core and each Cu(II) ion is in similar environments coordinated to two (O, N) donor sets as revealed from single-crystal X-ray diffraction studies. The coordination geometry can best be described as distorted square planar which could be judged using the τ_4 index, $\tau_4 = 360 - (\alpha + \beta)/141°$, where α and β are the two largest angles subtended by the ligand donor atoms in the four-coordinate complex. The average indexes for **3e** and **4e** were found to be 0.42 and 0.43 respectively, signifying a considerable distortion from an idealized square planar, D_{4h} geometry (τ_4=0.0) or idealized tetrahedral, T_d geometry (τ_4=1.0). The average Cu•••Cu distance between closest copper(II) ions in the complex **3e** is 4.48 Å. On the other hand, the single crystal X-ray analysis showed that each of the three Cu(II) centers in complex **4e** is strongly tetracoordinated to two N and two O atoms & weakly to two O atoms of the methoxy groups of the ligand, *N*,*N'*,O,O′-3, 3′-bis ((2-methoxyphenyl)-iminomethyl)-[1, 1’-biphenyl]-2, 2′-diol (**H_2L^3**). Generally, Cu–N & Cu–O bond lengths are (1.983 – 1.994) & (1.882 – 1.893) respectively, comparable to similar systems.

KEY WORDS: Biphenol, 2,6-dimethoxyaniline, 2,6-dimethylaniline, Dinucleating ligands Trinuclear copper(II) complexes, Magnetic susceptibility

1. Introduction

Recent years have witnessed an explosion of interests in the research of polynuclear complexes, not only because of their intriguing variety of architectures and multinuclear metals[1], but also because of their fascinating extraordinary properties in the fields of catalysis, metalloenzyme and magnetic materials[2–8]. In line with this, polynuclear copper complexes are studied for their interesting magnetic and spectral properties which can serve as potential models of biological systems in the characterization of the active sites of multicopper proteins [2,7,9,10] and biological activities such as antitumor, antiviral, and anti-inflammatory[11,12]. Currently, there are extensive studies on the synthesis and construction of the biphenol-based metal complexes, which are derived from 2, 2’-dihydroxy-[1, 1’-biphenyl]-3, 3’-dicarbaldehyde with 2, 6-dialkylanilines displaying interesting magnetic, electronic, and/or catalytic properties[13,14]. Among the various ligand modification reactions, salicylaldimine ligands derived from the condensation of 2,2'-dihydroxy-[1,1'] biphenyl -3,3'-dicarbaldehyde and diamines such as 2,6-diethylaniline, 2,6-dimethylaniline[3], and 2,6-diisopropylaniline represent an important series of chelating agents that have been used to synthesize mono-, di-, or polynuclear transition metal complexes. Copper(II) complexes, on the other hand, represent models of physical and chemical behavior of biological copper systems that mimic copper metalloproteins such as hemocyanin[15–17]. Polynuclear copper complexes with biphenol based ligands, in particular, have gained considerable interest because of their relevance to the fungal enzyme galactose, with recent progress in biomimetic model complexes which have been summarized in several excellent reviews[8,18–20]. Complexes with two or more metal centers have shown also promising efficiency in the field of catalysis mainly because of their cooperativity effect[5,21]. Each metal centers shown in **Scheme 1**, has tetradentate cavities coordinated to two N & O sites, leaving the metal centers coordinatively unsaturated, and thus room for further coordination [22] by exogenous ligands. In this paper we report the synthesis of biphenol-based N2O2 donor ligands (**H_2L^2**) and (**H_2L^3**), formed by the facile condensation of 2, 2’-dihydroxy-[1, 1’-biphenyl]-3, 3’-dicarbaldehyde (**c**) with 2-methoxy /2, 6-dimethylaniline and the corresponding trinuclear copper(II) complexes (**3e** and **4e**) (**Scheme 1)**. All the ligands and complexes were characterized by elemental analysis (EA) and spectroscopic techniques [21]. The variable temperature magnetic behavior and single crystal X-ray diffraction (SCXRD) of the two trinuclear complexes have also been described and the results have been compared with those of similar complexes reported in the literature

2. Experimental

2.1. Materials

All starting materials were reagent grade and purchased from commercial sources. 2,6-dimethylaniline and 2-methoxyaniline were purchased from Sigma Aldrich, Germany and used without further purification. Solvents were purified and degassed by standard procedures[18]. 2,2'-dihydroxy-[1,1'-biphenyl]-3,3'-dicarbaldehyde (**c**) was synthesized using literature procedure[23].

2.2. Synthesis

2.2.1. Synthesis of 3,3′-*bis*[(2,6-dimethyl-phenylimino)-methyl]-[1,1'] biphenyl-2,2'-diol (**H_2L^2**)

To a solution of 3,3′-diformyl-2,2’-dihydroxy-1,1′- biphenyl (**c**) (0.204 g, 0.843 mmol) in a mixed medium of toluene (10 mL) and EtOH (10 mL), 2,6-dimethylaniline (0.306 g, 2.53 mmol) was added dropwise in the presence of few drops of formic acid under magnetic stirring. The reaction mixture was refluxed for 10 hours using a Dean stark trap apparatus in which the water formed as a byproduct of the condensation reaction separated out. The volatiles were then removed under high vacuum and the residue was washed with cold methanol three times and dried under reduced pressure to give a yellow solid (**H_2L^2**). Yield: (0.289 g, 76 %). ^{1}H NMR ($CDCl_3$, 400 MHz, 25 °C): δ 13.2 (s, 2H, 2O$\underline{H}$), 8.39 (s, 2H, 2C$\underline{H}$N), 7.61 (dd, 2H, $^3J_{HH}$ = 8 Hz, $^4J_{HH}$ = 2 Hz, 2$C_6\underline{H}_3$), 7.32 (dd, 2H, $^3J_{HH}$ = 8 Hz, $^4J_{HH}$ = 2 Hz, 2$C_6\underline{H}_3$), 7.05–7.02 (m, 6H, 2$C_6\underline{H}_3(CH_3)_2$), 6.98 (t, 2H, $^3J_{HH}$ = 8 Hz, 2(2,6-$C_6\underline{H}_3(CH_3)_2$)), 2.25 (s, 12H, 2(2,6-$C_6H_3(C\underline{H}_3)_2$)). Anal. Calcd.for $C_{30}H_{28}N_2O_2$ (448.56): C, 80.33; H, 6.29; N, 6.25. Found: C, 80.54; H, 5.81; N, 6.12 . Uv–Vis(nm): 236, 341.

2.2.2. Synthesis of 3,3'-bis(2-methoxyphenyl)imino)methyl)-[1,1'-biphenyl]-2,2'-diol (**H_2L^3**)

To a solution of 3, 3′-diformyl-2, 2’-dihydroxy-1, 1′- biphenyl (**c**) (0.204 g, 0.843 mmol) in a mixed medium of toluene (10 mL) and EtOH (10 mL), 2-methoxyaniline (0.311 g, 2.53 mmol) was added dropwise in the presence of few drops of formic acid under magnetic stirring. The reaction mixture was refluxed for 10 hours using a Dean stark trap apparatus in which the water formed as a by product of the condensation reaction separated out. The volatiles were then removed under high vacuum and the residue was washed with cold methanol three times and dried under reduced pressure to give a yellow brown solid (**H_2L^3**). Yield: 0.257 g (68 %). ^1H NMR ($CDCl_3$, 400 MHz, 25 °C): δ 14.25 (s, 2H, 2O*H*), 8.51 (s, 2H, 2C*H*N), 7.61 (d, 2H, $^3J_{HH}$ = 8 Hz, $2C_6\underline{H}_3$), 7.45 (d, 2H, $2C_6\underline{H}_3$), 7.25–7.40 (m, 2H, $C_6\underline{H}_3$), 6.90–7.08 (m, 6H, C_6H_4), 6.8 (t, 2H, C_6H_4), 3.58 (s, 6H, $2(OC\underline{H}_3)$.)). Anal. Calcd.for $C_{28}H_{24}N_2O_4$ (452.50): C, 74.32; H, 5.35; N, 6.19 %. Found: C, 74.45; H, 5.72; N, 6.04 %. Uv–Vis(nm): 249, 341.

2.2.3. *Tris* [3, 3′-*bis* [(2, 6-dimethylphenyl) imino) methyl]-[1, 1'] - biphenyl-2, 2’-dioxo copper (II)] (**3e**)

A hot solution (50 °C) of $[Cu_2(OAc)_4(H_2O)_2]$ (0.334 g, 1.67 mmol)) in MeOH (10 mL) was added dropwise while stirring to a hot suspension (60 °C) of (3,3′-*bis*[(2,6-dimethylphenyl)imino)methyl]-[1,1']biphenyl-2,2'-diol (**H_2L^2**) (0.165 g, 0.368 mmol) in MeOH (10 mL). The reaction mixture was then refluxed for 12 hours in the presence of few drops of triethylamine, during which time the formation of precipitate was observed. The reaction was cooled to room temprature and concentrated under reduced pressure. The residue was dissolved in CH_2Cl_2 (40 mL), filtered over celite and the volatiles were removed under reduced pressure to give a brownish powder. Single-crystals of compound **3e** suitable for X-ray diffraction were grown by slow evaporation of a solution of acetonitrile and dichloromethane (1:1) at room temprature. Yield: 0.108 g (55 %). Anal. Calcd.for $C_{90}H_{78}Cu_3N_6O_6$(1530.26): C, 70.64; H, 5.14; N, 5.49 %. Found: C, 70.45; H, 5.22; N, 5.23 %. IR (KBr): ν(cm^{-1}): 3434 (w), 2960 (s), 2935 (s), 1601 (s), 1587 (s), 1545 (s), 1424 (s), 1169 (s), 747 (s), 519 (m). Uv–Vis(nm):230, 274, 310, 406.

2.2.4. *Tris* [3, 3’-*bis* ((2-methoxphenyl) imino) methyl)-[1, 1’-biphenyl]-2,2’-trioxo copper(II)] (**4e**)

A hot solution (50 °C) of [Cu_2 $(OAc)_4(H_2O)_2$] (0.131 g, 0.654 mmol) in MeOH (10 mL) was added dropwise while stirring to a hot suspension (60 °C) of 3, 3'-*bis* ((2-methoxyphenyl) imino) methyl)-[1, 1'-biphenyl]-2,2'-diol (0.164 g, 0.362 mmol) **(H_2L^3)** in MeOH (10 mL). The reaction mixture was then refluxed for 12 hours in the presence of few drops of triethylamine, during which time the formation of precipitate was observed. The reaction was cooled to room temprature and concentrated under reduced pressure. The residue was dissolved in CH_2Cl_2 (40 mL), filtered over celite and the volatiles were removed under reduced pressure to give dark green solid. Single-crystals of compound **4e** suitable for X-ray diffraction were grown by slow evaporation of a solution of acetonitrile and dichloromethane (1:1) at room temprature. Yield: 0.103 g (52 %). Anal. Calcd. for $C_{84}H_{66}Cu_3N_6O_{12}$ (1542.09): C, 65.42; H, 4.31; N, 5.45 %. Found: C, 65.58; H, 4.69; N, 5.48 %. IR (KBr): ν(cm^{-1}): 3437 (w), 2964 (s), 2931 (s), 1603 (s), 1588 (s), 1548 (s), 1424 (s), 1169 (s), 747 (s), 519 (m). Uv–Vis(nm):228, 275, 312, 405.

2.3. Methods and measurements

1H NMR and13C {1H} NMR spectra were recorded on Bruker 400 MHz and Bruker 500 MHz NMR spectrometers. Elemental Analysis was carried out on Thermo Finnigan FLASH EA 1112 SERIES (CHNS) Elemental Analyzer. Infrared spectra were recorded on a Perkin Elmer Spectrum one FT-IR spectrometer. The electronic spectra were recorded in dichloromethane using a Perkin Elmer Lamda 35 UV-Visible spectrophotometer. Mass spectrometry measurements were performed on a Micromass Q-Tof spectrometer. Cyclic voltammetry was performed at room temperature in dichloromethane under liquid nitrogen atmosphere, in a three-electrode cell connected to a Schlenk line. The counter electrode was a platinum wire of 1 cm2 apparent surface area. The reference was a saturated calomel electrode (SCE) separated from the solution by a bridge (4 ml) filled with a 0.1 M. Variable-temperature magnetic susceptibility measurements were performed on pulverized crystalline samples in the range 5 to 300 K with a Quantum Design MPMS-5 SQUID magnetometer. Magnetic data were corrected for the diamagnetism of the sample holder and diamagnetism of the sample using Pascal's constants[24]. The EPR measurements were made with a Varian model 109C E-line X-band spectrometer fitted with a quartz Dewar for measurements at 77 K. The spectra were calibrated using tetracyanoethylene (tcne) (g = 2.0037).

2.4. X-ray crystal structure determination

X-ray diffraction data were collected on a Bruker P4 diffractometer equipped with a SMART CCD detector and crystal data collection and refinement parameters are summarized in Tables 3 and 4. Single-crystal X-ray data for **3e** and **4e** were collected at 100K and 150K respectively. The structures were solved using direct methods and standard difference map techniques, and were refined by full-matrix least-squares procedures on F2 with SHELXTL (Version)[2]. CCDC-1400845 (for 3e) and CCDC- 1432509 (for 4e) contain the supplementary crystallographic data. These data can be obtained free of charge from the Cambridge Crystallographic Data center via www.ccdc.cam.ac.uk/data_request/cif.

3. Results and discussion

3.1. Synthesis of ligands 3, 3′-*bis*-((R)-iminomethyl)-(1,1')-biphenyl-2,2'-diol, where R = 2,6-$Me_2C_6H_3$ (H_2L^2), 2- $OMeC_6H_4$ (H_2L^3)

The tetradentate chelating ligands, $\mathbf{H_2L^n}$ **(**n = 2, 3**)** used in this work were prepared in high yields by the condensation reaction of 2, 2’-dihdroxy-[1, 1-biphenyl]-3, 3-dicarbaldehyde (**c**) (**Scheme 1**) with three equivalents of 2,6-dialkylaniline in a mixed medium of toluene and EtOH (1:1) at about 60 °C in the presence of catalytic amount of formic acid [25–27]. The condensation reaction was confirmed by the complete disappearance of C*H*O proton ^{1}HNMR resonance peak at 11.43 ppm and the appearance of–C*H*N−proton peak[28] at 8.40 ppm in the ligand $\mathbf{H_2L^2}$ [6,29]. Information gained from HRMS, IR & UV-Vis[6] spectras indicate that both ligands possess four coordination sites (two imino–N and two biphenolic–O atoms). When fully deprotonated, they provide N_2O_2 tetradentate environments which could encapsulate two metal ions and bridge two other similar ligands to form a trinuclear structure. Both $\mathbf{H_2L^2}$ and $\mathbf{H_2L^3}$ are soluble in organic solvents such as chloroform, dichloromethane, ethanol, methanol or other low-polar organic solvents.

3.2. Synthesis of trinuclear copper(II) complexes, [M (3,3′-*bis*-((R)-iminomethyl)-(1,1')-biphenyl-2,2'-dioxo)]$_3$, M =Cu(II), R = 2, 6-$Me_2C_6H_3$ (3e) and M =Cu (II), R = R = 2-$OMe_2C_6H_4$ (**4e**)

The ligands were subsequently employed for the synthesis of corresponding trinuclear complexes according to the synthetic pathways summarized in **Scheme 1**[17,30]. The complexes were prepared by the reaction of methanolic solution of $\mathbf{H_2L^n}$ with excess $[Cu_2(OAc)_4(H_2O)_2]$ in the presence of triethylamine[9,31,32]. Complexes **3e** & **4e** were isolated using the appropriate workup as brownish and dark green colored solids with 55 and 52 % yields respectively. The synthesized compounds are thermally stable, air and moisture insensitive on storage under ordinary conditions. They exhibit good solubility in common non polar organic solvents. The molecular identity and geometry of complexes **3e** and **4e** were elucidated by the single crystal X-ray crystal structure determination. Good elemental analysis data comparable with the calculated ones were obtained for the complexes. Solvent of crystallization was detected in the single crystal X-ray structures of complexes. The solvents were used for the crystal growth and believed to be incorporated in the voids or lattices, holding partly the three dimensional crystal structures.

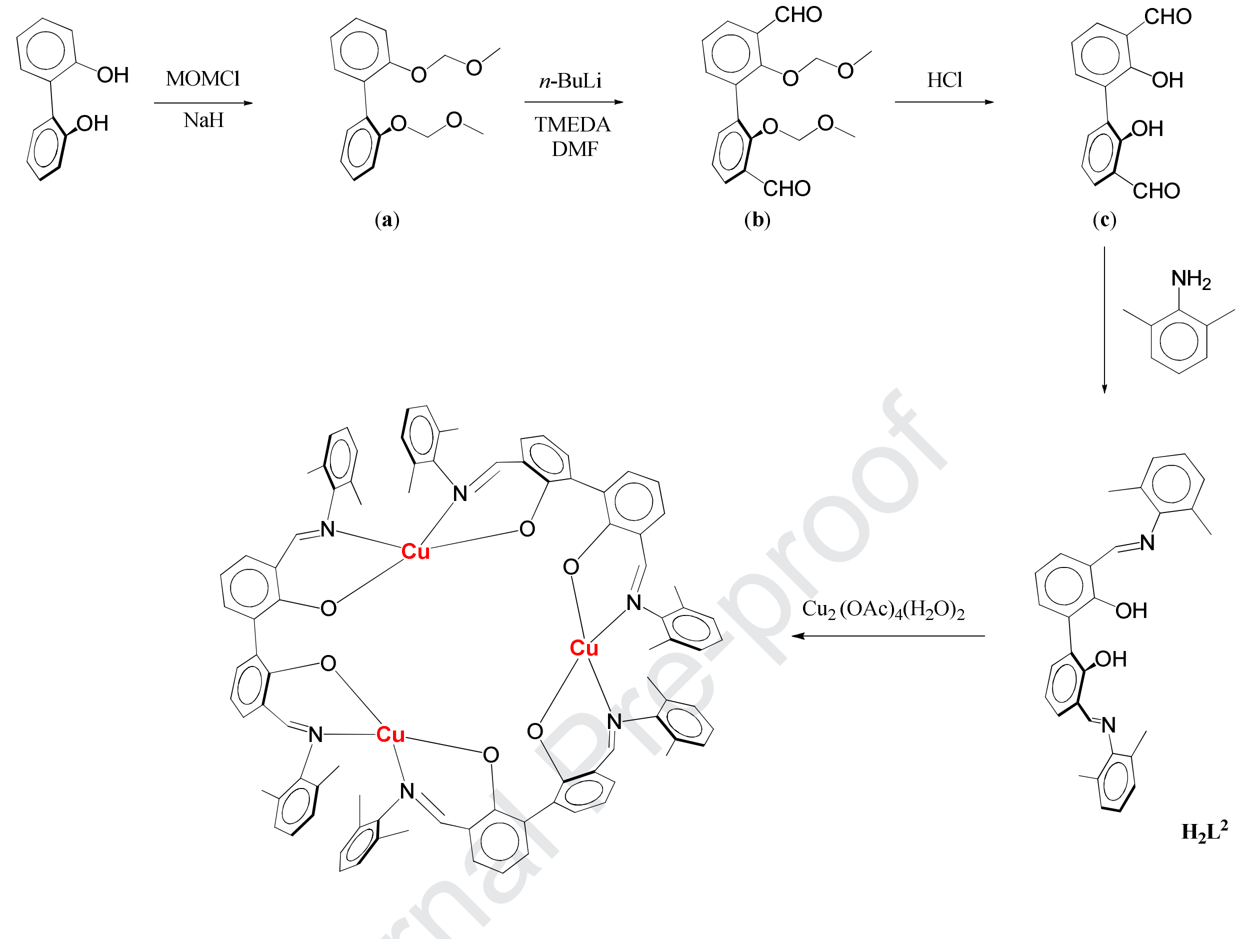

M = Cu(II) (**3e**)

Scheme 1. Synthesis of ligand **H_2L^2** and the corresponding trinuclear copper(II) complex **3e.**

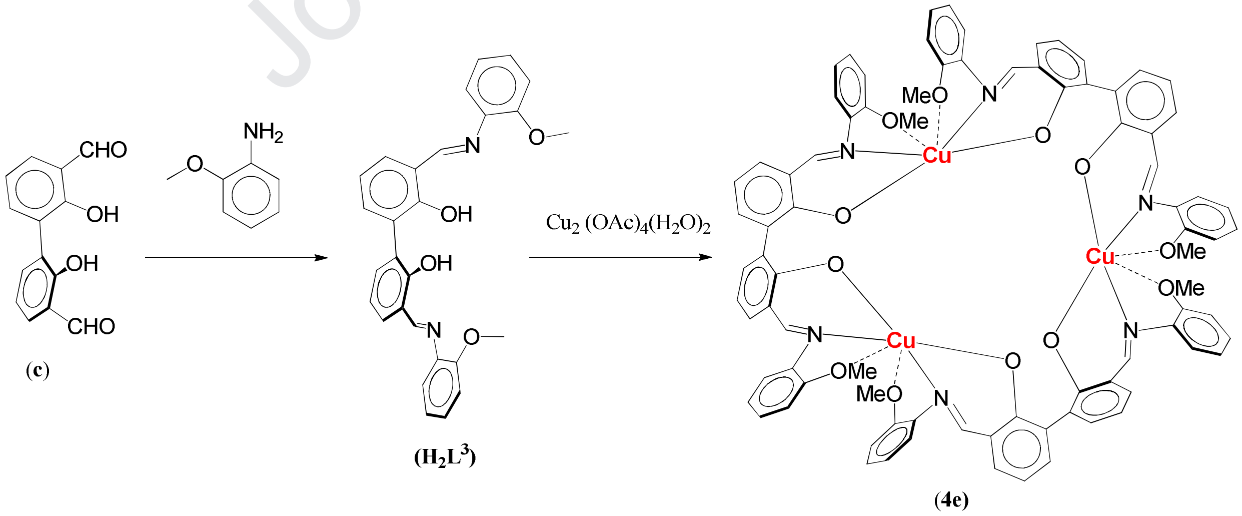

Scheme 2. Synthesis of ligand **H_2L^3** and the corresponding trinuclear copper(II) complex **4e.**

3.3. Spectroscopic characterizations

3.3.1. FTIR Spectra

In the FT-IR spectra of the ligands $\mathbf{H_2L^2}$ and $\mathbf{H_2L^3}$, strong absorption band at ν 3440 cm^{-1} assignable to O-H stretching is observed[33,34]. The FT-IR spectra of complex **4e** also show the retention of this band in the said region due to the absorption of coordinated H_2O[25,36]. However, this band is absent in the spectra of **3e** which shows the absence of coordinated H_2O and complete deprotonation and coordination of OH to the Cu(II) core[27]. The azomethine *ν*(C=N) absorption band and the biphenolic C−O stretching bands are observed at 1618 cm^{-1} and 1205 cm^{-1} in the spectra of $\mathbf{H_2L^2}$ respectively [28,37]. Strong band at 1427 cm^{-1} is assigned to *ν*(C=C) biphenyl stretching vibrations [16]. Up on complexation, the positions of C=N, C−O, and C=C vibrations were shifted to lower frequencies 1602 , 1201, 1425 cm^{-1} respectively and their intensities were changed[38]. This confirms the coordination takes place through the azomethine nitrogen C=N and the deprotonated biphenol oxygen C−O leading to lower electron density on the azomethine and oxygen of the ionized hydroxyl C−O of the biphenol ring[28]. The ν(C−O) shifts to lower frequencies because of the high electronegative oxygen of C−O which exerts an electron withdrawing effect reducing the C−O bond electron density and consequently weakening the force constant[28,39]. Similarly, the azomethine C=N stretching and the biphenolic C−O stretching bands were observed at 1617 cm^{-1} and 1208 cm^{-1} in the spectra of $\mathbf{H_2L^3}$ respectively [28,37]. These bands were shifted to lower frequencies in the corresponding complex **4e** to 1603 cm^{-1} and 1174 cm^{-1} respectively (Table 1S, Supplementary data).

3.3.2. Electronic spectra

The electronic spectra of ligands ($\mathbf{H_2L^2}$ and $\mathbf{H_2L^3}$) in CH_2Cl_2 showed strong absorption band in the region 228–230 nm, attributable to $\pi \rightarrow \pi^*$ transition in –C=N– bond[34,40]. This band was shifted to higher wave length 274–310 nm (red shift) up on complexation[33]. The band in the region 274–275 nm is due to $n \rightarrow \pi^*$ transition of the azomithine group[17]. This may involve the transfer of lone pair electrons of azomethine-N to the lowest unoccupied orbitals (LUMO) of the imine double bond. Upon complexation, it undergoes a blue shift in the complexes[32].

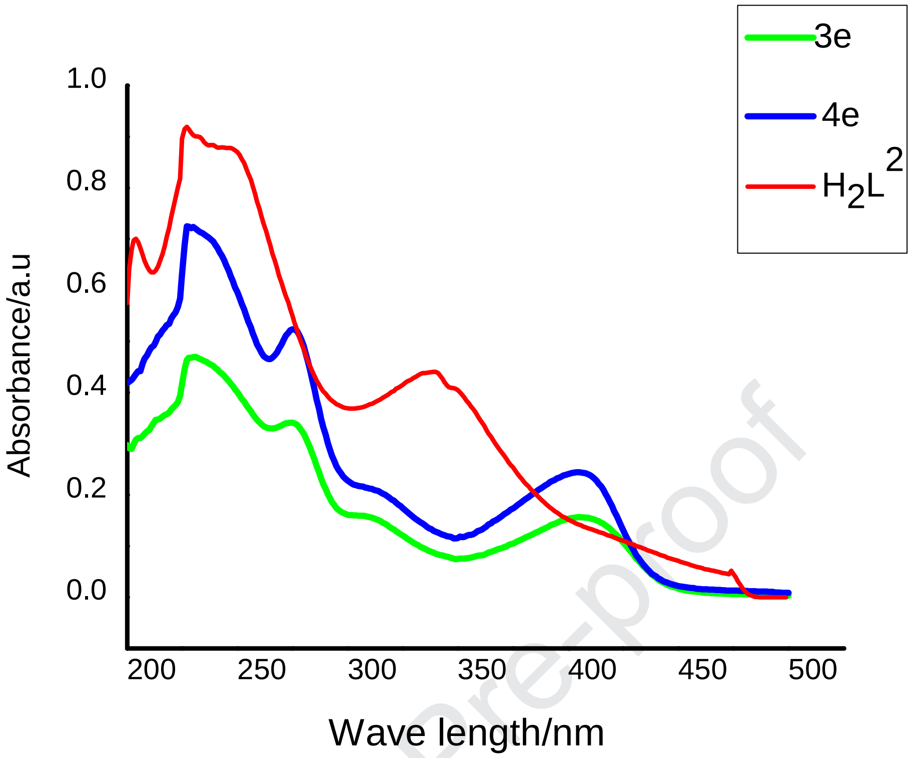

Fig. 1. UV-visible spectra of the trinuclear copper complex, **3e**, **4e** and $\mathbf{H_2L^2}$ in CH_2Cl_2.

This confirms the coordination of Cu(II) to the ligand through the azomethine nitrogen. In the spectra of the trinuclear Cu(II) complexes, the position and intensity of the absorption band that is characteristic of the ligand appeared to be modified with respect to those of the free ligands. The bands observed in the region 310–312 nm could be assigned as the metal-to-ligand charge (MLCT) transfer transition[36] which might be attributed to the metal d→ligand π* charge-transfer transions (Table 2) (supporting info)[27]. The relatively intense broad bands in the regions 405–406 nm are attributed to the Cu^{II}–O biphenolate ligand– to –metal charge transfer transitions[41]. These bands probably incorporate both d-d and charge transfer transitions[42]. The spectra of complexes **3e** and **4e** show no apparent bands within the 900-500 nm range, although it is very likely that the expected d-d transitions are masked by the broad and intense charge transfer bands[6,41].

3.4. Cyclic voltammetry

Cyclic voltammograms of the trinuclear copper(II) complex **3e** was measured in order to gain insight about the tendency of the new trinuclear copper(II) complexes to undergo oxidation–reduction. Experiments were carried out in CH_2Cl_2 (1 mM) solution of compound **3e** with 0.1 M (n-Bu_4N)(ClO_4) as the supporting electrolyte under liquid nitrogen atmosphere.

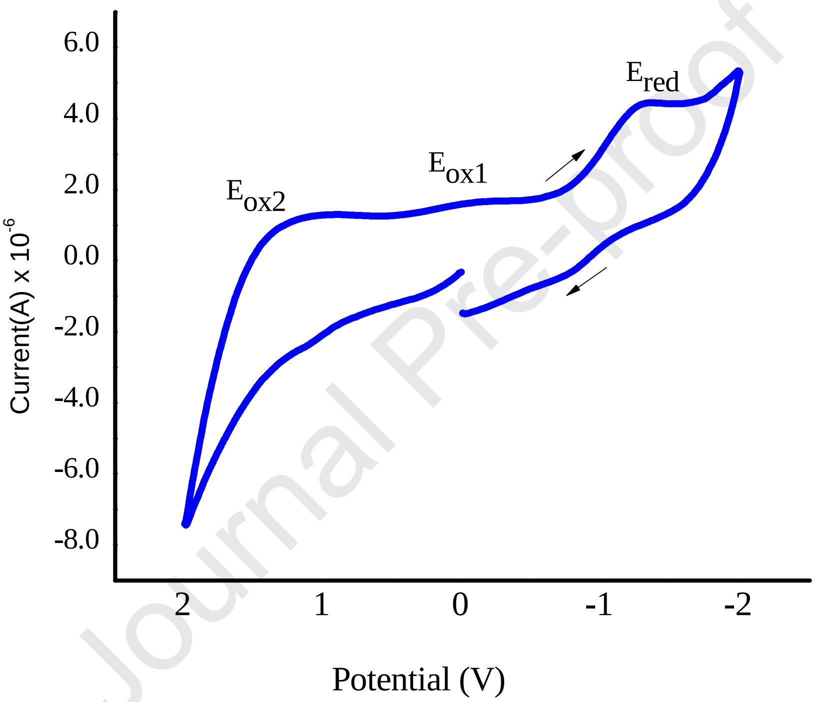

Fig. 2. Cyclic voltammogram of **3e** (1.0 mM) in CH_2Cl_2 with 0.1 M (n-Bu_4N)(ClO_4) obtained on a glassy carbon electrode at a scan rate of 100mVs^{-1}.

The anodic region (Figure 2) of **3e** shows quasi reversible (E_{ox1}) and (E_{ox2}) oxidation processes at anodic potential peak values: E_{ox1} = 0.164 V, E_{ox2} = 1.33 V respectively[43]. In the negative direction, the cyclic voltammogram also shows quasireversible reduction signal at the cathodic potential peak: E_{red} = -1.30 V. Based on comparison with the previous works , the oxidations could be assigned to biphenolate-ligand centered processes ($BiphO_2^{2-} \rightarrow BiphO_2^{\bullet -} \rightarrow BiphO_2\!:$) while the reduction ($E_{red}$) corresponds to the Cu^{II}/Cu^{I}) couple [14,28,44].

Thus, the anodic peaks are assigned to the sequential one-electron oxidations, $BiphO_2^{2-} \rightarrow BiphO_2^{\bullet\,-}$ (E_{ox1}), $BiphO_2^{\bullet\,-} \rightarrow BiphO_2^{:}$ (E_{ox2}), while the cathodic peak is assigned to reduction involving (Cu^{II}/Cu^{I})(E_{red})[43]. The quasireversible redox waves suggest that each oxidation/reduction is followed by a rearrangement, which is both electronic and structural.

The Cu^{II} ions are high spin while the Cu^{I} ions are low spin, thus, reduction of Cu^{II} may initially produce a high-spin Cu^{I} species, which presumably undergoes a rapid spin change[7]. The electrochemical properties of complex **4e** is found to be analogous with that of complex **3e** and not presented here. Finally, it should be noted that comparison of our results with reported data is delicate in case where different solvents have been employed, since it is obvious that the potentials are markedly dependent on the solvent.

3.5. Magnetic properties

3.5.1. Magnetic Susceptibilities

The magnetic properties of the trimers **3e** and **4e** were measured using a SQUID magnetometer over the temperature range 5–300 K at 100 Oe[1]. The temperature dependence of $\chi_M T$ (χ_M being the magnetic susceptibility per Cu_3 entity) for complexes **3e** and **4e** are shown in Figures 4 and 5 respectively[42]. At room temperature, the $\chi_M T$ ($\chi_M T = \mu eff^2/8$) value (0.958 cm^3 K mol^{-1}) of complex **3e** is substantially lower than that expected for three uncoupled Cu(II) ions (1.125 cm^3 K mol^{-1}, considering $g = 2$[1]). Plots of the magnetic susceptibility and reciprocal magnetic susceptibility for **3e** and **4e** are given in Fig. 3 and 6 respectively[8,42]. The Curie–Weiss behavior of **3e** indicates a linear relation of the reciprocal magnetic susceptibility curve at higher temperatures (100–300 K) with a Curie constant C = 0.236 cm^3 mol^{-1} K and Weiss-constant, $\theta = -8.26$ K and a small anomaly is observed only at the lowest temperatures[33]. The compound reveals a magnetic behavior which is characteristic of antiferromagnetic spin coupling[34,45]. The $\chi_M T$ values decrease gradually with lowering the temperature, from 0.958 cm^3 mol^{-1} K at 300 K to 0.256 cm^3 mol^{-1} K at 5.8 K [43]. Below 100 K to 50 K the decrease observed on the $\chi_M T$ values is slightly less pronounced, tending to the expected plateau, characteristic of an $S = 1/2$ system resulting from an antiferromagnetically coupled trinuclear Cu(II) compound. Below 50 K the magnetic susceptibility shows a new rapid decrease, which can only be attributable to antiferromagnetic intramolecular interactions [9,46]. Similarly, at room temperature, the χ_mT value of complex **4e** is 0.987 cm^3 K mol^{-1}, when lowering the temperature to 25 K, this value decreases to 0.61 cm^3 K mol^{-1}. The Curie–Weiss behavior of **4e** indicates a linear relation of the reciprocal magnetic susceptibility curve at higher temperatures (100–300 K) with a Curie constant C = 0.182 cm^3 mol^{-1} K and Weiss-constant, θ = -5.05 K, which also suggests the presence of weak antiferromagnetic interactions among the trimeric Cu(II) ions[47].

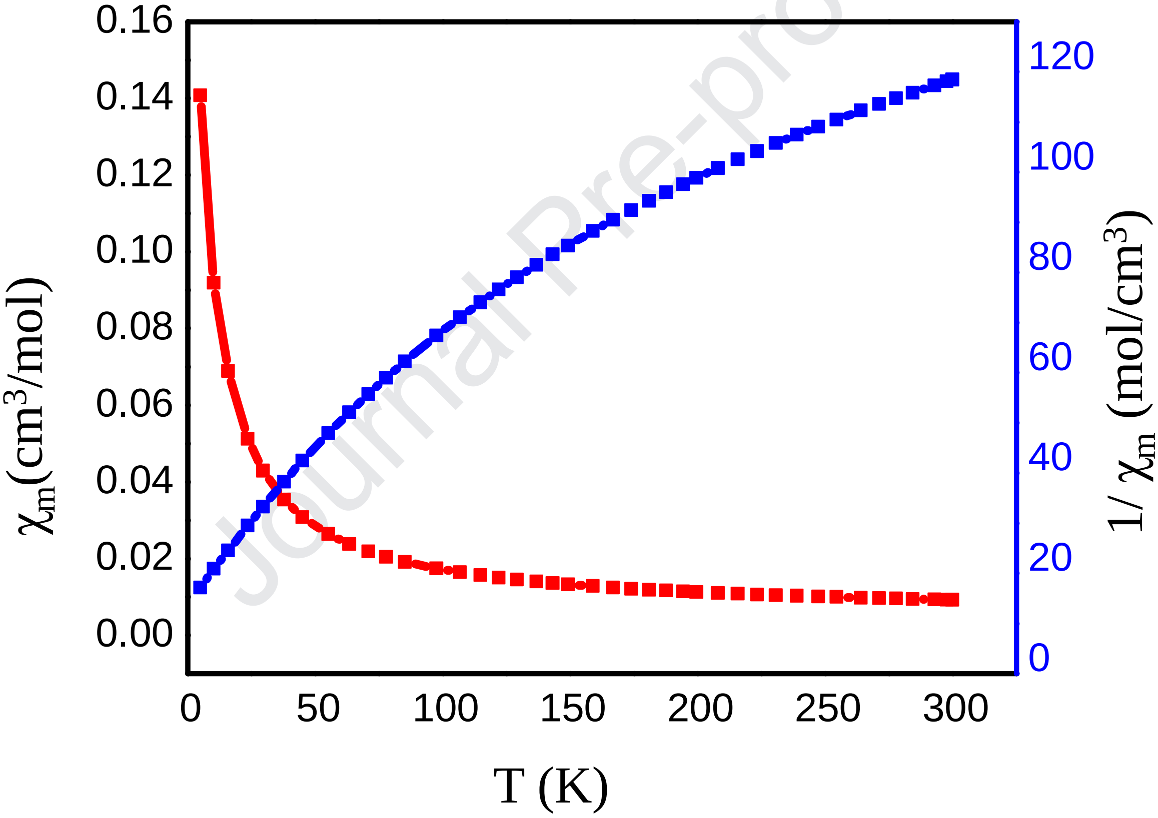

Fig. 3. Temperature dependence of χ_m and1/χ plot for complex **3e** at 100 Oe. The solid line is the best exponential fit of the experimental data.

The χ_MT value decreases sharply and reaches to a minimum value of 0.45 cm^3 K mol^{-1}at 6 K [48]. Furthermore, the effective magnetic moments of complexes **3e** and **4e** at room temperature are 2.79 and 2.71 B.M. respectively[4], which is less than the spin only value of Cu(II), 3.87 B.M., calculated ($[4S(S + 1)]^{1/2}$; S = 3(1/2)) for three uncoupled spin 1/2 centers [29,44,47,49].

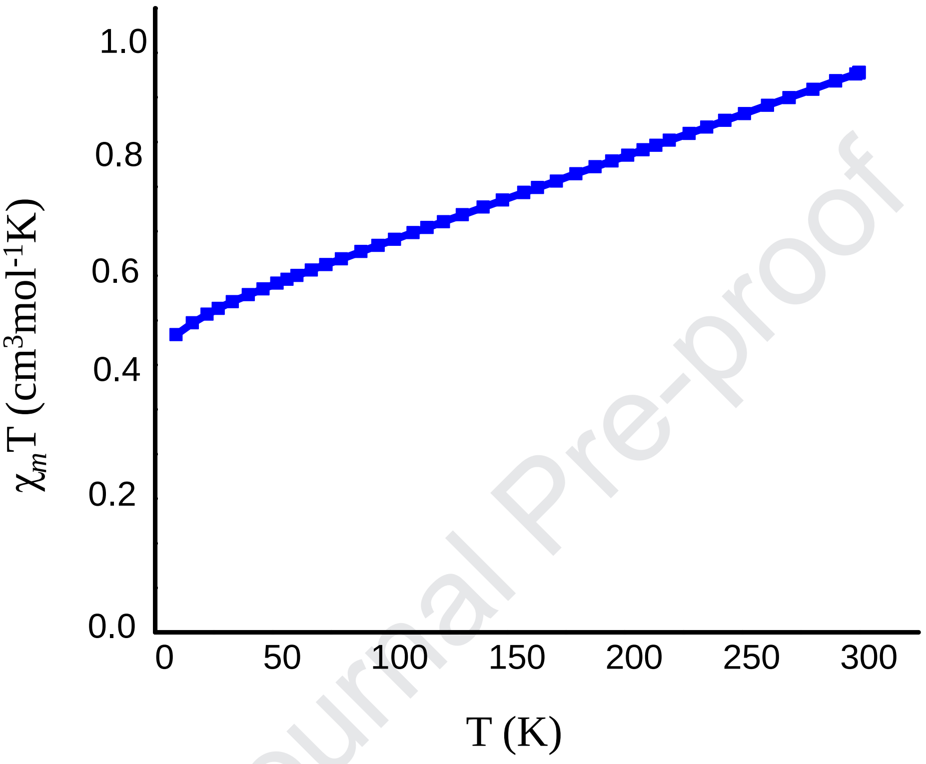

Fig. 4. Temperature dependence of χ_mT for complex **3e** at 100 Oe. The solid line is the best exponential fit of the experimental data

To quantify the magnetic interactions (J) in complexes **3e** and **4e**, it is shown that the three Cu(II) ions of each [$Cu_3N_2O_2$] system occupy vertices of an equilateral triangle as the three Cu(II) centres are equivalent[12,46,50]. Each Cu(II) ions should interact with the two adjacent Cu(II) ions similarly as the Cu(II)•••Cu(II) distances are equivalent[51]. The magnetic exchange pathway for each pair involves the biphenyl-O and N- bridging group of the derived Schiff base ligand. In order to investigate the magnetic behavior of these trinuclear complexes, an isotropic Heisenberg–Dirac–Van Vleck (HDVV) Hamiltonian was used in the approach[34].

$$\hat{H} = -J_{12}S_1S_2 - J_{13}S_1S_3 - J_{23}\, S_2S_3 \qquad (1)$$

Since the three copper atoms of the [$Cu_3N_2O_2$] unit define a quasi-equilateral triangle, the three Cu^{II} ions can be considered equivalents, thus $J_{12} = J_{13} = J_{23} = J_{CuCu}$ & Eq.(1) can be written in the form $\hat{H} = -J_{CuCu}(S_1S_2 - S_1S_3 - S_2S_3)$.

The magnetic susceptibility deduced from the Hamiltonian is given in Eq. (2), where N, g, β and k have their usual meanings.

$$\chi_m T = (Ng^2\beta^2 T/4KT)[1 + 5\exp(3J/2KT)]/(1+\exp(3J/2KT)) \qquad (2)$$

The best fitting was obtained for **3e** with an isotropic coupling constant $J_{CuCu} = -15$ cm^{-1} and $g_{CuCu} = 1.99$, assuming a temperature-independent paramagnetic correction of $\chi TIP = 2.4 \times 10^{-3}$ cm^3 K mol^{-1}, Magnetic impurity (MI) = 0.18 % (Table 2). Similarly, the best agreement with the experimental data was obtained for **4e** with $J_{CuCu} = -18$ cm^{-1} and $g_{CuCu} = 1.99$, assuming a temperature-independent paramagnetic correction of $\chi TIP = 2.81 \times 10^{-3}$ cm^3 K mol $^{-1}$, Magnetic impurity (MI) = 0.16 % [14,47] (Table 2). Thus both complexes show weak antiferromagnetic interactions (Table 3)[6,29]. Generally, the decrease in the magnitude of $\chi_M T$ with decreasing system temperature for these types of complexes could result from several factors such as intramolecular M–M interactions between the Cu(II) centres, [Cu•••Cu 4.48Å (**3e**) and Cu•••Cu 4.54 Å (**4e**)], significant spin-orbit coupling inherent to the Cu(II) ions as well as non-negligible intermolecular interactions (4.84 Å) even at room temperature [6,10,14,47].

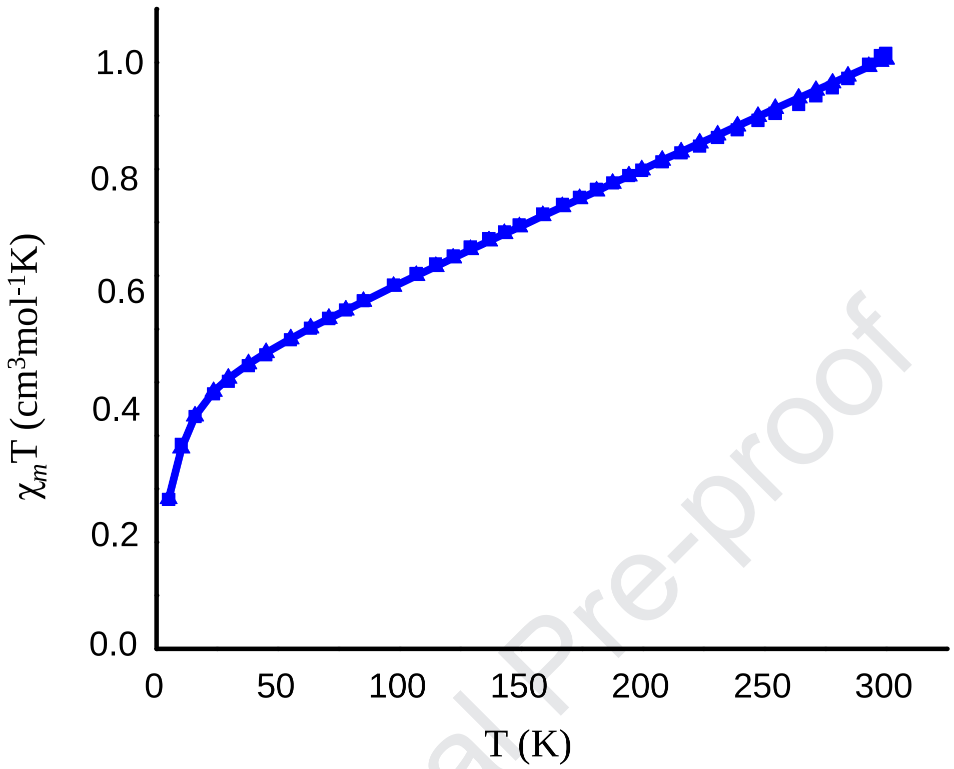

Fig. 5. Temperature dependence of χ_mT for complex **4e** at 100 Oe. The solid line is the best exponential fit of the experimental data.

The antiferromagnetic coupling observed in the complexes can also be explained from the magneto-structural correlations established for biphenol linkers[52]. These correlations established that magnetic coupling strongly depend on the Cu–O, the Cu–Cu separation and to small extent on the geometries around the coupling. In the present case, the exchange coupling (J) can be explained in terms of the geometrical distortions that affect the copper coordination spheres.

The core structures found in complexes **3e** and **4e** are reasonably similar with previously reported[45] trinuclear Cu(II) complexes where three Cu(II) ions of each [$Cu_3N_2O_2$] system occupy alternate corners of a cube[53].

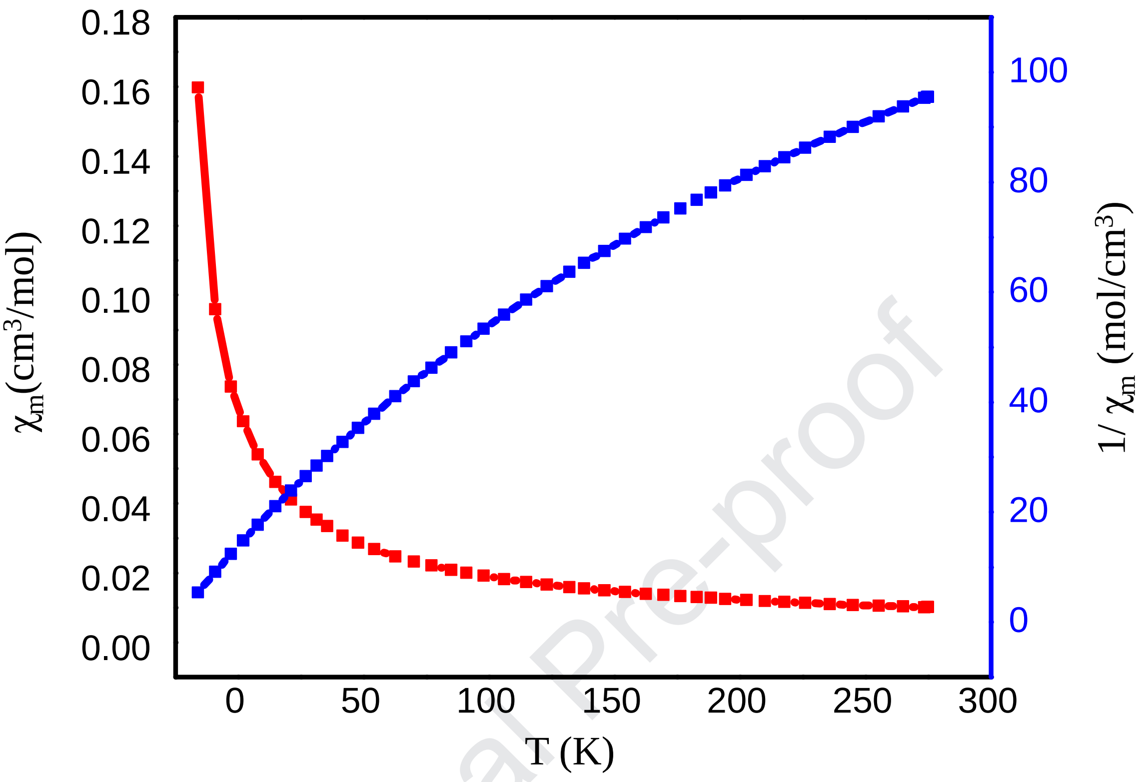

Fig. 6. Temperature dependence of χ_m and 1/χ_m for complex **4e** at 100 Oe. The solid line is the best exponential fit of the experimental data.

Therefore, each Cu(II) ion is connected to the adjacent Cu(II) ion through one [$Cu_3N_2O_2$] group and one biphenoxyl bridging group. The molecular structure also shows that the aromatic linkers connect the Cu(II) centers in an equilateral fashion[54]. It is obvious that the single electron of the Cu^{2+} in the dx^2-y^2 orbital always participates in a strong magnetic structural correlations of complexes of such type show that larger Cu•••Cu angles favor larger antiferromagnetic contributions[55].

In triangular complexes, where the arrangement of the magnetic centers corresponds to equilateral triangles, the three cores show antiferromagnetic coupling which give rise to spin frustration effects [34]. The spin frustration requires two conditions: (a) a highly symmetrical triangle and (b) a degenerate ground state.[56] The existence of spin frustration for this kind of complexes is most likely studied by means of EPR spectra at very low temperatures when only the degenerate S = 1/2 states are populated[56]. One of the signatures of spin frustration is the appearance of g values equal or close to 2.00[34].

3.5.2. Electron paramagnetic spectroscopy

The EPR spectra of complexes **3e** and **4e** was recorded as polycrystalline powder at 100K with X-band microwave magnetic field. The spectrum of **4e** at 100K shows a single absorption band observed approximately at g_{iso} = 2.12., whereas the EPR spectra of **3e** shows g value centered at g_{iso} = 2.11 with no hyperfine splitting (A)[57], indicating antiferromagnetic interaction between copper ions in both complexes[58,59]. The isotropic nature of the signal is probably due to the exchange narrowing resulting from nearby Cu units in the crystal lattice[34].

Thus, EPR of both complexes at the lowest temperatures reveal only one unpaired electron on the whole trimer molecule which can be related to a doublet (S = 1/2) species and to a higher spin state generated by spin coupling within units becoming thermally populated at higher temperatures[51]. They show unresolved single resonances peaks, due to exchange coupling between the copper ions[8,34]. As can be noticed, the line width at 100 K (**Fig. 7 & 8**) is small, but no anisotropy of g or hyperfine coupling with the Cu nuclei can be detected[61]. On the other hand, a proper consideration of this interaction should in principle take into account three Cu nuclei with different hyperfine couplings and the simultaneous presence of the two isotopes $_{63}$Cu and $_{65}$Cu, in comparable natural abundance [36]. Generally, the results indicate that the ground state of both **3e** and **4e** is a doublet state[42]. The same explanation was suggested to account for the EPR features of a similar trinuclear copper[62]. It is interesting to note that the g factor components are similar to those measured recently at low temperature for a spin-frustrated symmetric trinuclear copper complex, which clearly display the features of the quartet state at high temperature [56].

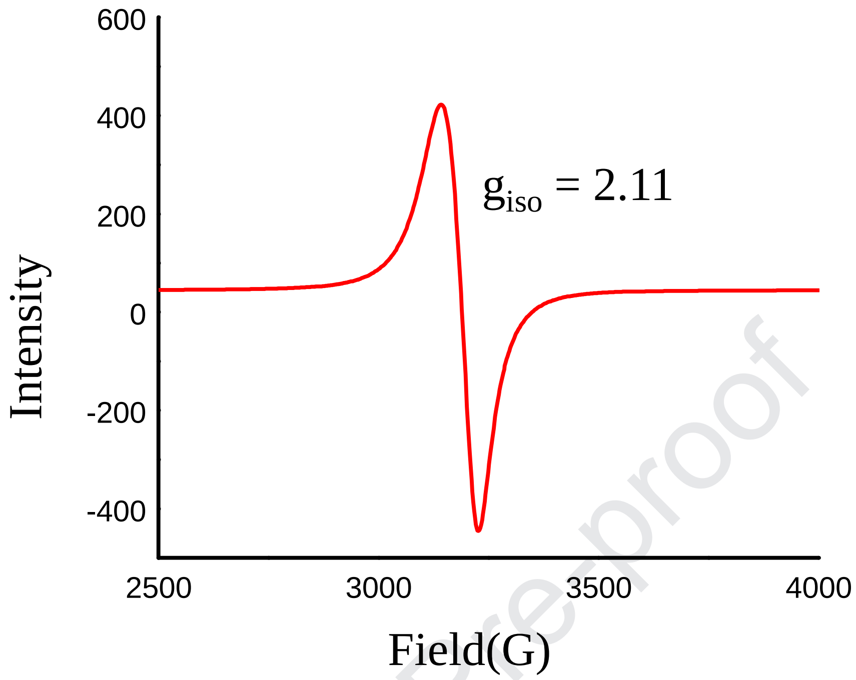

Fig. 7. Polycrystalline X-band EPR spectra for complex **3e** at 100 K.

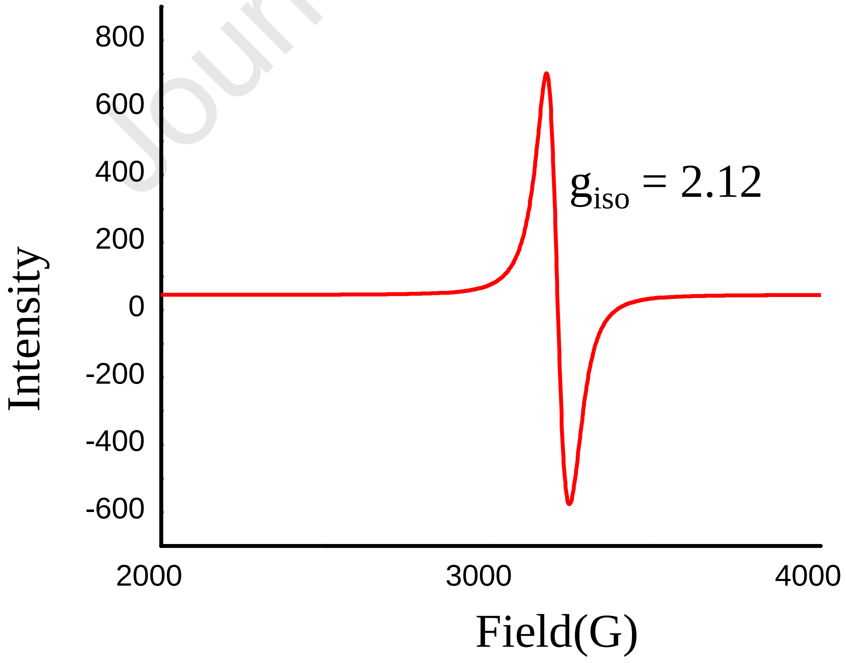

Fig. 8. Polycrystalline X-band EPR spectra for complex **4e** at 100 K.

Table 1

Magnetic data for **3e** and **4e** at 300 K.

S.No	Metal complex	Obs.χ_M(cm^{3}mol^1)	1/χ(cm^{3}mol)	χ_MT(cm^{3}mol^{-1}K)	$\mu_s(_B)$	$\mu_{s+l}(_B)$	Obs.$\mu_{eff}(\mu_B)$
1	**3e**	0.010	98.15	0.987	3.87	5.19	2.71
2	**4e**	0.011	90.9	0.958	3.87	5.19	2.79

Table 2

List of magnetic fitting parameters in complexes **3e** and **4e**.

S.No.	Metal complex	$g_{cu(II)}$	J_{CuCu}(cm^{-1})	Temperature Independent Paramagnetism(10^{-3}cm^{3}mol)	Magnetic impurity (%)
1	**3e**	1.99	-15	2.40	0.18
2	**4e**	1.99	-18	2.81	0.16

3.6. Single Crystal X-ray diffraction

X-ray quality crystals were readily obtained for **3e** and **4e** through slow diffusion of CH_3CN into a CH_2Cl_2 solution of the complex

The single crystal X-ray diffraction data and experimental details for complexes **3e** and **4e** are available in **Table 3** and their structures along with selected bond lengths and angles are given in **Table 4**.

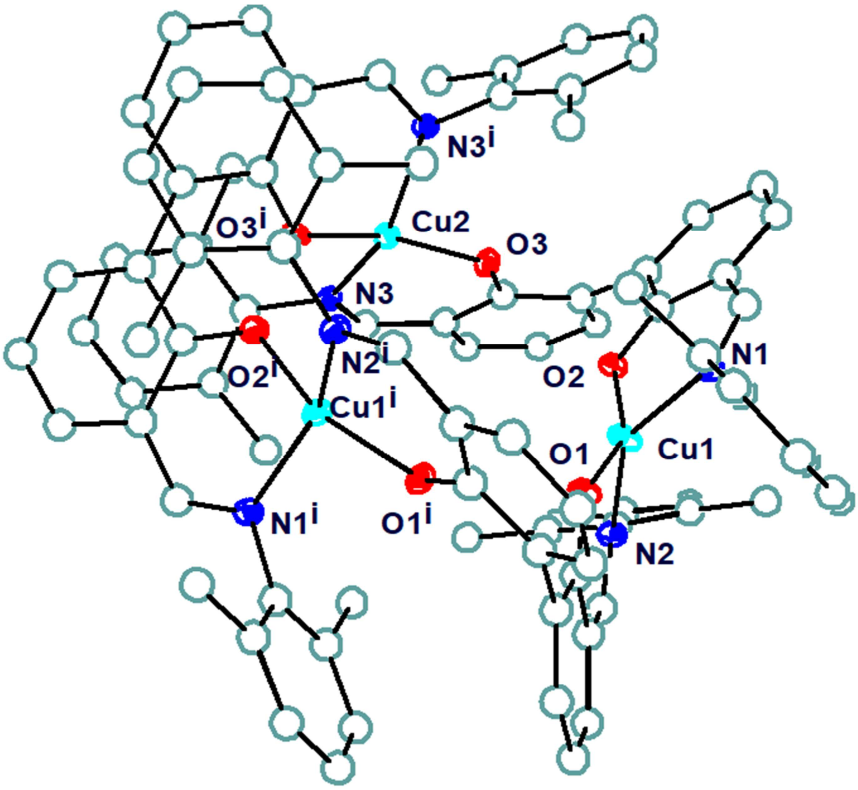

Fig. 9. Molecular structure of **3e** with thermal ellipsoids plotted at the 50 % probability level.

Description of the crystal structures of **3e** and **4e**

Each Cu(II) ion in complex **3e** is coordinated through the lone pairs of biphenolate-O and the imine-N atoms of the ligand $\mathbf{H_2L^2}$[36]. The Cu(II) ion coordination polyhedron in **3e** is formed by the ligation of imine –N and biphenolate-O atoms[29]. The geometry around each Cu(II) atom can be best described as distorted square planar where Cu(II) centers are in similar environments coordinated to two (O, N) donor sets[52,63]. The distorted nature of the geometry around each Cu(II) atoms can be judged from the τ_4 index,

$$\tau_4 = 360 - (\alpha + \beta)/141°$$

where α and β are the two largest angles subtended by the ligand donor atoms in the four-coordinate complex.

The average indexes for **3e** and **4e** were found to be 0.42 and 0.43 respectively, signifying a considerable distortion from an idealized square planar, D_{4h} geometry (τ_4=0.0) or idealized tetrahedral, T_d geometry (τ_4=1.0)[64]. Cu–O and Cu–N bond distances are in the respective ranges 1.870(7) –1.890(4) and 1.985(4)–1.975 Ǻ, which are consistent with literature values [42,56]

Complexes **3e** and **4e** are isomorphous and crystallized in the monoclinic space group C2/c. All Cu_1, Cu_2 and Cu_3 in **4e** display distorted square planar geometry, being surrounded by two adjacent imine–N atoms and two –O atoms [7]. For each Cu(II) ions, the two oxygen atoms come from the deprotonated biphenol oxygen atom –O and two nitrogen atoms from imine of the ligand[34]. In addition to strong coordination in **4e** with two (O, N) donor sets, each Cu(II) ion is weakly coordinated with two O atoms from the two ortho methoxy group.

Both complexes **3e** and **4e** are trimeric and are centrosymmetric due to the presence of an inversion center in the middle of each molecule[53]. In complex **4e**, 2, 2-biphenol-based Schiff base complex Cu1-O1-N1-N2 and $Cu1^i$-$O1^i$-$N1^i$-$N2^i$ are formed by the two azomithine-N and two biphenolate-O ligand $\mathbf{H_2L^3}$ moieties and three cu(II) ions[51]. Crystallographically equivalent atoms have equivalent bond lengths and bond angles. The structure of **4e** consists of a trinuclear unit containing a symmetrical $Cu_3N_6O_6$ core with each Cu(II) ion located on the corner of an equilateral triangle[3].

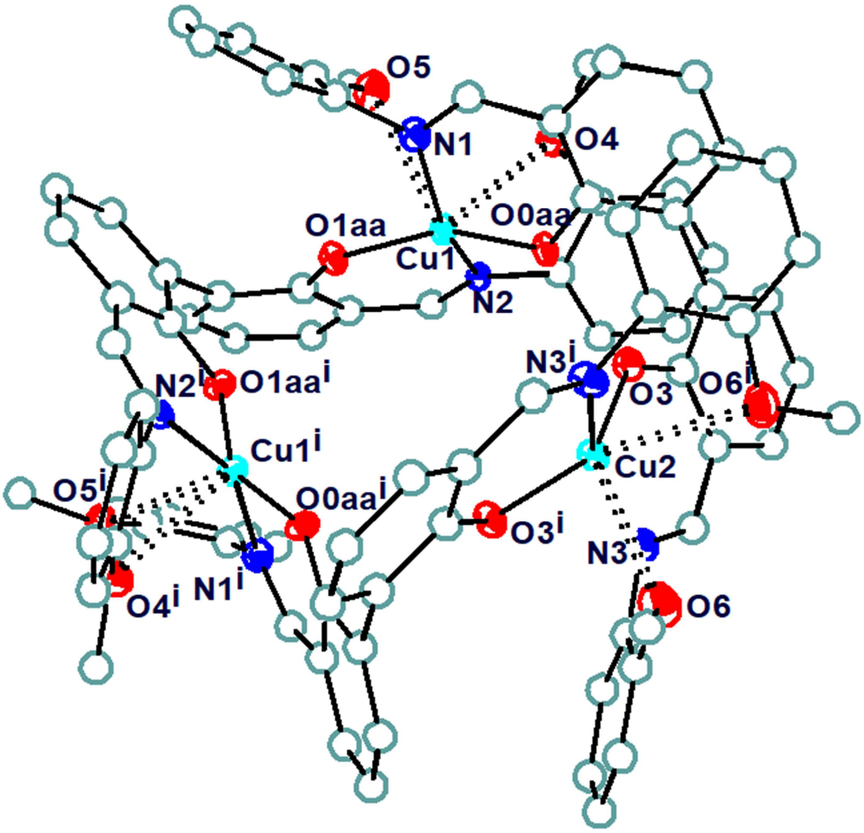

Fig. 10. Molecular structure of **4e** with thermal ellipsoids plotted at the 50 % probability level.

The ORTEP drawing and atom-labeling scheme of complex **4e** is shown in **Fig. 10** and selected geometrical parameters are given in Table **4**. There is no direct covalent linkage between Cu(II) ions and the trigonal arrangement of the biphenyl linkers at each Cu(II) ion leads these metals to be separated by a distance of 4.804(1) Å[12]. Each Cu(II) ions is coordinated by two nitrogens and alkoxy oxygen donor from the ligand [Cu(1)–N(1) 1.983(5) Å, Cu(1)–N(2) 2.013(5) Å, Cu(1)–N(3) 1.976(4) Å and Cu(1)–O(1) (1.938(3) Å][34,52]. The geometry at each Cu (II) ion may be considered as pseudo octahedral, being surrounded in the equatorial plane by two nitrogens and two oxygens from different ligands [Cu(2)– N(4) 1.988(5) Å, Cu(2)–O(1) 1.957(3) Å], and at axial positions by two oxygen atoms O(9) from methoxy group on the ligand which is at significantly longer distance, 2.602(4) Å). Complexes (**3** & **4**)**e** represent the first family which are characterized spectrometrically and structurally[51].

Table 3

X-ray crystallographic data for compounds **3e**. 2(C_7H_8).H_2O and **4e**. 2(CH_2Cl_2)

Data	**3e**. 2(C_7H_8). H_2O	**4e.** 2(CH_2Cl_2)
Formula	$C_{104}H_{96}Cu_3N_6O_7$	$C_{86}H_{70}Cl_4Cu_3N_6O_{12}$
Crystal system	Monoclinic	Monoclinic
Formula weight	1530.25	1542.0938
Space group	*C*2/c	*C*2/c
a/ Å	14.693(3)	25.215(60)
b/ Å	15.287(3)	15.002(3)
c/ Å	21.242(5)	20.902(5)
α/◦	90	90
β/◦	105.573(3)	109.399(3)
γ/◦	90	90
V/Å	84.69(3)	74.58(3)
Z	4	4
temperature (K)	100	150
radiation (λ, Å)	0.71070	0.71070
ρ(calcd.), g cm^{-3}	1.359	1.525
θ max, deg.	25.00	25.00
No. of data	7469	6573
No. of parameters	553	499
$R1^a$	0.0543	0.0808
$wR2^b$	0.118	0.2490
GOF	1.079	1.099

[a] $R1=\Sigma|F_o|-|F_c|/\Sigma F_o$

[b] $wR2 = \{[\Sigma w(F_o-F_c)^2]/[\Sigma w(F_o)^2]\}^{1/2}$

Table 4

Selected bond lengths (Ǻ) and angles (◦) of complexes **3e** and **4e**

Complex	**3e**	Complex	**4e**
Cu(1)−O(2)	1.870(2)	Cu(1)-O(1AA)	1.899(3)
Cu(1)−O(1)	1.887(2),	Cu(1)−O(0AA)	1.910(3),
Cu(1)−N(2)	1.975(3),	Cu(1)−N(2)	1.976(4),
Cu(1)–N(1)	1.975(3)	Cu(1)−N(1)	1.984(4)
Cu(2)–O(4)	1.873(2),	Cu(2)−O(3)	1.896(3)
Cu(2)−O(3)	1.873(2)	Cu(2)−O(3)^i	1.896(3)
Cu(2)–N(3)	1.975(3)	Cu(2)−N(3)	1.964(4)
Cu(2)–N(4)	1.975(3)	Cu(2)−N(3)^i	1.964(4)
Cu(3)−N(5)	1.985(3)	Cu(3)−O(3)	1.896(3)
Cu(3)−N(6)	1.985(3).	Cu(3)−O(3)^i	1.896(3)
Cu(3)−O(5)	1.873(2),	Cu(3)−N(3)	1.964(4)
Cu(3)−O(6)	1.873(2)	Cu(3)−N(3)^i	1.964(4)
O(2)−Cu(1)−O(1)	152.30(10),	O(1AA)−Cu(1)−O(0AA)	148.87(13)
O(2)−Cu(1)−N(2)	92.90(10)	O(1AA)−Cu(1)−N(2)	93.17(14)
O(1)−Cu(1)−N(2)	94.90(10)	O(0AA)−Cu(1)−N(2)	94.17(14)
O(2)−Cu(1)−N(1)	94.71(10)	O(1AA)−Cu(1)−N(1)	93.99(14)
O(1)−Cu(1)−N(1)	94.72(10)	O(0AA)−Cu(1)−N(1)	92.61(14)
N(2)−Cu(1)−N(1)	143.38(11)	N(2)−Cu(1)−N(1)	153.84(15)
O(3)−Cu(2)−O(3$^{\mathbf{i}}$)	159.11(14)	O(3)−Cu(2)−O(3)^i	140.08(18)
O(3)−Cu(2)−N(3)	91.79(10)	O(3)−Cu(2)−N(3)	94.24(14)
O(3)−Cu(2)−N(3$^{\mathbf{i}}$)	94.01(10),	O(3)−Cu(2)−N(3)^i	94.64(14)
O(3)−Cu(2)−N(3)	94.01(10	O(3^i)−Cu(2)−N(3)	94.64(14)
O(3$^{\mathbf{i}}$)−Cu(2)−N(3)	91.79(10),	O(3)^i−Cu(2)−N(3)^i	94.24(14)
N(3)−Cu(2)−N(3$^{\mathbf{i}}$)	147.57(15).	N(3)−Cu(2)−N(3)^i	153.8(2)

4. Conclusion

In summary, we have synthesized the first example of trinuclear copper(II) complexes as revealed by the spectrometric and spectroscopic techniques. The structure and coordination geometry of complexes (**3** and **4**)**e** were deduced from the Single Crystal X-ray crystallographic studies. The complexes show weak antiferromagnetic interaction. Evidence for intramolecular interaction was obtained from the fitting of experimental magnetochemistry with the theoretical ones which give coupling constant (J) values characteristics of antiferromagnetic interaction. The trimeric, paramagnetic and redox active nature of the complexes probe good future magnetic (as single molecule magnets), catalytic or antibiological applications. The study for catalytic applications of the complexes is underway in our lab

.

Conflicts of interest

The authors declare no conflict of interest

Acknowledgments

The Authors would like to express their gratitude for the financial support from the Department of Science and Technology (EMR/2014/000254), New Delhi, India and Ministry of Education, Ethiopia. The authors gratefully acknowledge the central Facility, Department of Chemistry, IIT Bombay, Mumbai, India, for the Single Crystal X-ray crystallographic characterization and Professor P. Ghosh, Department of Chemistry, IIT Bombay for his technical support in this study.

Appendix A. Supplementary data

^{1}H NMR, ^{13}C{^{1}H} NMR, IR, HRMS, elemental analysis data of 3,3′-*bis*[(2,4,6-trimethyl-phenylimino)-methyl]-[1,1']biphenyl-2,2'-diol (**H_2L^1**), 3,3′-*bis*[(2,4,6-trimethyl-phenylimino)-methyl]-[1,1']binaphthalenyl-2,2'-diol (**H_2L^2**) and the trinuclear copper (**3e & 4e)** complexes ,CIF file giving X-ray crystallographic data can be found in the journal webpage. This material is available free of charge via journal webpage.

References

[1] J. W.Shin, A. R. Jeong, S. Y. Lee, C.Kim, S. Hayami, K.S. Min, J. Chem. Soc., Dalton. Trans. 45 (2016) 14089.

[2] S.W. Jong, R.J. Ah, H. Shinya, M. Dohyun, M.S. Kil, Inorg. Chem. Front. 2 (2015) 763–770.

[3] A.M. Abdulghani, A.J., Khaleel, Bioinorg. Chem. Appl. 2013 (2013) 1–14.

[4] G.T.M. Rebecca, A. Joy, H. Arman, S. Xiang. Inorganica Chim. Acta. 394 (2013) 220–228.

[5] R.M. Clarke, T. Storr, J. Chem. Soc., Dalton. Trans. 43 (2014) 9380–9391.

[6] L. Zhang, W. Gao, Q. Wu, Q. Su, J. Zhang, Y. Mu, J. Coord. Chem. 66 (2013) 3182–3192.

[7] T.K.P. Oindrila Das, E. Zangrando, Inorganica Chim. Acta. 362 (2009) 3617–3623.

[8] L. Cheng, J. Wang, X. Zhang, S. Gou, L. Fang, Inoche. 47 (2014) 144–147.

[9] H. Nairita, M.Shuvankar, J.Arpita , S.Hazel A, M.Sankasekhar, Rsc Adv. 8 (2018) 7315-7329.

[10] L. Botana, J. Ruiz, J.M. Seco, A.J. Mota, A. Rodríguez-Diéguez, R. Sillanpää, E. Colacio, J. Chem. Soc., Dalton. Trans. 40 (2011) 12462–12471.

[11] N. Novoa, F. Justaud, P. Hamon, T. Roisnel, O. Cador, B. Le Guennic, C. Manzur, D. Carrillo, J.R. Hamon, Polyhedron 86 (2015) 81–88.

[12] E. Salvadeo, L. Dubois, J. Latour, Coord. Chem. Rev. 374 (2018) 345–375.

[13] G. Ambrosi, M. Formica, V. Fusi, L. Giorgi, A. Guerri, M. Micheloni, P. Paoli, R. Pontellini, P. Rossi, Inorg. Chem. 46 (2007) 309–320.

[14] T.C. Davenport, T.D. Tilley, J. Chem. Soc., Dalton. Trans. 44 (2015) 12244–12255.

[15] A.C.W. Leung, J.K.H. Hui, J.H. Chong, M.J. MacLachlan, J. Chem. Soc., Dalton. Trans. 26 (2009) 5199–5210.

[16] M. Maria. C, G. Michele , S. Laura, B.Giuseppe, M. Enrico, P.Roberto, Z.Giorgio, C. Luigi, J. Chem. Soc., Dalton. Trans. 14 (2004) 2192–2201.

[17] S. Halder, S. Dey, C. Rizzoli, P. Roy, Polyhedron 78 (2014) 85–93.

[18] A. Hazari, L. K. Das, R. M. Kadam, A. Bauzá, J. Chem. Soc., Dalton. Trans. 44 (2015) 3862–3876.

[19] I. Bratko, M. Gómez, J. Chem. Soc., Dalton. Trans. 42 (2013) 10664–10681.

[20] Z. Chen, X. Wang, Y. Li, Z. Guo, Inorg. Chem. Commun. 11 (2008) 1392–1396.

[21] W. Plass, B. Kintzel, M. Bo, Chem. Commun. 54 (2018) 12934–12937.

[22] H.V.R. Dias, H.V.K. Diyabalanage, M.A. Rawashdeh-omary, M.A. Franzman, M.A. Omary, J. Am. Chem. Soc. 125 (2003) 12072–12073.

[23] J.M. Grill, J.H. Reibenspies, S.A. Miller, J. Organomet. Chem. 690 (2005) 3009–3017.

[24] S. Ganguly, R. Sanyal, R. Mondal, Eur. J. Inorg. Chem. (2014) 5874-5884

[25] M. S. Jana, S. Dey, J. L. Priego, R. Jiménez-Aparicio, T. K. Mondal, P. Roy, Polyhedron 59 (2013) 101–106.

[26] P. Gajewski, M. Renom-Carrasco, S.V. Facchini, L. Pignataro, L. Lefort, J.G. De Vries, R. Ferraccioli, U. Piarulli, C. Gennari, European J. Org. Chem. 2015 (2015) 5526–5536.

[27] X. Gong, Y.Y. Ge, M. Fang, Z.G. Gu, S.R. Zheng, W.S. Li, S.J. Hu, S. Bin Li, Y.P. Cai, CrystEngComm. 13 (2011) 6911–6915.

[28] B. Ortiz, S.M. Park, Bull. Korean Chem. Soc. 21 (2000) 405–411.

[29] H. Shimakoshi, S. Hirose, M. Ohba, T. Shiga, H. Okawa, Y. Hisaeda, Bull. Chem. Soc. Jpn. 78 (2005) 1040–1046.

[30] K. Mochizuki, J. Takahashi, Y. Ishima, T. Shindo, Inorganica Chim. Acta. 400 (2013) 151–158.

[31] J. Sun, Q. Shan, L. Chen, W. Chen, X. Zhang, C. Yang, Inorg. Chem. Commun. 108 (2019) 107506.

[32] S.H. and K.S.M. Jong Won Shin , Ah Rim Jeong , Sun Young Lee, C. Kim, J. Chem. Soc., Dalton. Trans. 45 (2016) 14089–14100.

[33] H.D. Bian, J.Y. Xu, W. Gu, S.P. Yan, P. Cheng, D.Z. Liao, Z.H. Jiang. Polyhedron 22 (2003) 2927–2932.

[34] B. Sarkar, M. S. Ray, M.G.B. Drew, A. Figuerola, C. Diaz, A. Ghosh, Polyhedron 25 (2006) 3084–3094.

[35] F. Cuenú, J. Londo, J. Eduard , R. Abonia , R. F. D.Vries, J. Mol. Struct.1152 (2018) 163-176

[36] S. Saha, A. Sasmal, C. Roy Choudhury, C.J. Gómez-Garcia, E. Garribba, S. Mitra, Polyhedron 69 (2014) 262–269.

[37] A. Jozwiuk, Z. Wang, D.R. Powell, R.P. Houser, Inorganica Chim. Acta. 394 (2013) 415–422.

[38] A. Kendel , S.Miljani, D. Kontrec, Z. Soldin , N. Gali J. Mol. Struct. 1107 (2020) 127783

[39] M. Arefian, M. Mirzaei, H. Eshtiagh-Hosseini, J. Mol. Struct. 1156 (2018) 550–558.

.[40] Q. Zhou , R. Miao , D. Wang , R. Huang, J. Mol. Struct. 1206 (2020) 127688

[41] J. Sanmartín, M.R. Bermejo, A.M. García-deibe, O.R. Nascimento, L. Lezama, Å. Bond, J. Chem. Soc., Dalton. Trans. (2002) 1030–1035.

[42] J.M. Jirı Kamenıcek , V. Petrıcek , A. Kurecka , B. Kalinska, Polyhedron 26 (2007) 535–542.

[43] R. Shakya, A. Jozwiuk, D. R. Powell ,R. P. Houser, Inorg. Chem. 48 (2009) 4083–4088.

[44] A. Hazari, L.K. Das, R.M. Kadam, A. Bauzá, A. Frontera, A. Ghosh, J. Chem. Soc., Dalton. Trans. 44 (2015) 3862–3876.

[45]. M. Korabik, T. Lis, J. Lisowski, J. Chem. Soc., Dalton. Trans. 45 (2016) 15586–15594.

[46] L. Cheng, J. Wang, X. Zhang, S. Gou, L. Fang, Inorg.Chem.Commun. 47 (2014) 144–147.

[47] N. Fukita, M. Ohba, T. Shiga, Y. Ajiro, J. Chem. Soc., Dalton. Trans. (2000) 64–70.

[48] A. A. Khandar, J. White, T. Taghvaee-Yazdeli, S.A. Hosseini-Yazdi, P. McArdle, Inorganica Chim. Acta. 400 (2013) 203–209.

[49] G. Pascu, C. Deville, E. Cli, L. Guenée, C. Besnard, K.W. Krämer, S. Liu, S. Decurtins, F. Tuna, E.J.L. Mcinnes, R.E.P. Winpenny, A.F. Williams, J.Chem.Soc.,Dalton.Trans. 43 (2014) 656–662.

[50] M. Maghami, F. Farzaneh, J. Simpson, A. Moazeni, Polyhedron 73 (2014) 22–29.

[51] L. Jiang, D. Zhang, J. Suo, W. Gu, J. Tian, X. Liu, S. Yan, J. Chem. Soc., Dalton. Trans. 45 (2016) 10233–10248.

[52] G. V Baryshnikov, B.F. Minaev, A.T. Baryshnikova, H. Ågren, Chemical physics 491 (2017) 48-55.

[53] L. Rigamonti, A. Forni, M. Sironi, A. Ponti, A.M. Ferretti, C. Baschieri, A. Pasini, Polyhedron 145 (2018) 22–34.

[54] F.T. Iers, Inorg. Chem. Front. 2 (2015) 725–730.

[55] Z. Qi, J. Wu, C. Liu, R. Wang, Y. Sun, Chinese Sci. Bull. 51 (2006) 1421–1425.

[56] E.T. Spielberg, A. Gilb, D. Plaul, D. Geibig, D. Hornig, D. Schuch, A. Buchholz, A. Ardavan, W. Plass, Inorg. Chem. 54 (2015) 3432–3438.

[57] A.N. Gusev, V.F. Shul, E.A. Zamnius, M. Ricci, V. V Minin, G.G. Aleksandrov, I.L. Eremenko, W. Linert, Inorganica Chim. Acta. 430 (2015) 120–124.

[58] C. Karthick, P. Gurumoorthy, M.A.I. Musthafa. J. Cood .Chem. 67 (2014) 37–41.

[59] C. Mukherjee, U. Pieper, E. Bothe, V. Bachler, E. Bill, P. Chaudhuri, D.- Mu, Inorg. Chem.47 (2008) 8943-8956

[60] P. Kopel, S. Èermáková, K. Dole, B. Kaliñska, Polish J.Chem. 81 (2007) 327–335.

[61] M. Casarin, C. Corvaja, C. Nicola, D. Falcomer, L. Franco, M. Monari, L. Pandolfo, C. Pettinari, F. Piccinelli, P. Tagliatesta,V.Uni, R. Scientifica, I. Roma, Inorg. Chem. 43 (2004) 5865–5876.

[62] M. Roy, A. Adhikary, T. Debnath, A.K. Das, R. Mondal, Polyhedron 60 (2019) 46–52.

[63] M. Jayendran, P.M.S. Begum, M.R.P. Kurup, J. Mol. Struct. 1206 (2020) 127682.

[64] L. Yang, D.R. Powell, R.P. Houser, J. Chem. Soc., Dalton. Trans. 955 (2007) 955–964.

High lights of the paper entitled "Synthesis, Crystal Structure and Magnetic Properties of New Trinuclear Copper (II) Complexes with Biphenol–based dinucleating ligands".

- ✓ A comprehensive study on structural and magnetic descriptions were performed for new trinuclear copper (II) complexes.
- ✓ The complexes show antiferromagnetic property that also provide clue for the designing and synthesis of ferromagnetic complexes
- ✓ Tetradentate N2O2 ligands derived from 2,2-biphenyl carbaldehyde and 2, 2-methoxy/2-methyl aniline form distorted square planar trinuclear copper complexes
- ✓ Trinuclear metal centers each with tetradentate cavities coordinated to two N & O sites resulted in coordinatively unsaturated complex
- ✓ Complexes with two or more metal centers have shown promising efficiency in the field of catalysis mainly because of their cooperativity effect

The author declares no conflict of interest.